Aminoguanidine reduces diabetes-associated cardiac fibrosis

FERNANDO MAGDALENO[1,2], CHUCK CHRISTOPHER BLAJSZCZAK[2], CLAUDIA LISETTE CHARLES-NIÑO[1,3], ALMA MARLENE GUADRÓN-LLANOS[1], ALAN OMAR VÁZQUEZ-ÁLVAREZ[1], ALEJANDRA GUILLERMINA MIRANDA-DÍAZ[4], NATALIA NIETO[2], MARÍA CRISTINA ISLAS-CARBAJAL[4] and ANA ROSA RINCÓN-SÁNCHEZ[5]

[1]Department of Physiology, University Center of Health Sciences, Guadalajara University, Guadalajara, Jalisco 44340, Mexico; [2]Department of Pathology, College of Medicine, University of Illinois at Chicago, IL 60612, USA; [3]Department of Microbiology and Pathology; [4]Institute of Experimental and Clinical Therapeutics, Department of Physiology; [5]Institute of Molecular Biology and Gene Therapy, Department of Molecular Biology and Genomics, University Center of Health Sciences, Guadalajara University, Guadalajara, Jalisco 44340, Mexico

Received January 30, 2019; Accepted May 31, 2019

DOI: 10.3892/etm.2019.7921

Abstract. Aminoguanidine (AG) inhibits advanced glycation end products (AGEs) and advanced oxidation protein products (AOPP) accumulated as a result of excessive oxidative stress in diabetes. However, the molecular mechanism by which AG reduces AGE-associated damage in diabetes is not well understood. Thus, we investigated whether AG supplementation mitigates oxidative-associated cardiac fibrosis in rats with type 2 diabetes mellitus (T2DM). Forty-five male Wistar rats were divided into three groups: Control, T2DM and T2DM+AG. Rats were fed with a high-fat, high-carbohydrate diet (HFCD) for 2 weeks and rendered diabetic using low-dose streptozotocin (STZ) (20 mg/kg), and one group was treated with AG (20 mg/kg) up to 25 weeks. *In vitro* experiments were performed in primary rat myofibroblasts to confirm the antioxidant and antifibrotic effects of AG and to determine if blocking the receptor for AGEs (RAGE) prevents the fibrogenic response in myofibroblasts. Diabetic rats exhibited an increase in cardiac fibrosis resulting from HFCD and STZ injections. By contrast, AG treatment significantly reduced cardiac fibrosis, α-smooth muscle actin (αSMA) and oxidative-associated *Nox4* and *Nos2* mRNA expression. *In vitro* challenge of myofibroblasts with AG under T2DM conditions reduced intra- and extracellular collagen type I expression and *Pdgfb*, *Tgfβ1* and *Col1a1* mRNAs, albeit with similar expression of *Tnfα* and *Il6* mRNAs. This was accompanied by reduced phosphorylation of ERK1/2 and SMAD2/3 but not of AKT1/2/3 and STAT pathways. RAGE blockade further attenuated collagen type I expression in AG-treated myofibroblasts. Thus, AG reduces oxidative stress-associated cardiac fibrosis by reducing pERK1/2, pSMAD2/3 and collagen type I expression via AGE/RAGE signaling in T2DM.

Correspondence to: Dr Ana Rosa Rincón-Sánchez, Institute of Molecular Biology and Gene Therapy, Department of Molecular Biology and Genomics, University Center of Health Sciences, Guadalajara University, Sierra Mojada 950, Building 'Q' Third floor, Col. Independencia, Guadalajara, Jalisco 44340, Mexico
E-mail: anarosarincon@yahoo.com.mx

Abbreviations: AOPP, advanced oxidation protein products; αSMA, α-smooth muscle actin; AG, aminoguanidine; AGEs, advanced glycation end products; COL1A1, collagen type 1 α 1; eNOS, endothelial nitric oxide synthase; ECM, extracellular matrix; HFCD, high-fat, high-carbohydrate diet; IL-6, interleukin-6; MAPK/ERK, mitogen-activated protein kinase/extracellular signal-regulated kinase; NADPH, nicotinamide adenine dinucleotide phosphate; Nox4, NADPH oxidase 4; NO, nitric oxide; Nrf2, nuclear factor (erythroid-derived 2)-like 2; PDGF, platelet-derived growth factor; RAGE, receptor for advanced glycation end products; ROS, reactive oxygen species; STAT3, signal transducer and activator of transcription 3; STZ, streptozotocin; TGFβ, transforming growth factor β; TNFα, tumor necrosis factor α; T2DM, type 2 diabetes mellitus; UCPs, uncoupling proteins

Key words: AG, collagen type I, oxidative stress, STZ, AGEs, RAGE, diabetes, cardiac fibrosis

Introduction

Diabetes is a metabolic disorder of carbohydrates, proteins and lipids that contributes to development of cardiac fibrosis. It is predicted that the number of people with diabetes in the world could reach up to 592 million by the year 2035 (1). Thus, there is a pressing need to develop therapeutic interventions to attenuate diabetes and its associated cardiac fibrosis. Unfortunately, the molecular mechanisms responsible for cardiac fibrosis in type 2 diabetes mellitus (T2DM) are not well understood.

The literature suggests that accumulation of advanced glycation end products (AGEs), that crosslink with extracellular matrix (ECM) proteins, transduce fibrogenic signals through generation of reactive oxygen species (ROS) and activation of the receptor for AGEs (RAGE). In addition, activation of transforming growth factor β (TGFβ)/SMAD signaling may activate fibroblasts to induce deposition of structural ECM

proteins. Thus, activation of several distinct but overlapping pathways promotes diabetes-associated cardiac fibrosis (2).

Experimental induction of T2DM in animal models is essential to understand the oxidant stress and fibrogenic signals in T2DM (3). In this context, Streptozotocin (STZ), a preferential toxic compound of β cells, has been used for a long time in rodents to induce DM2 and to observe complications of the human form of the disease (4,5). High-fat, high-carbohydrate diet (HFCD) has been used to induce insulin resistance in combination with STZ, to reduce the compensatory capacity of β-cells facing insulin hypersecretion, resulting in hyperglycemia (6). Therefore, this combined model of HFCD-fed/STZ-treated rats is one of the best that simulates the progression of the natural disease and the typical metabolic characteristics of individuals at higher risk of developing T2DM.

Animal models of diabetes have revealed that aminoguanidine (AG), a known inducible nitric oxide synthase (iNOS) inhibitor, prevents diabetes-associated cardiovascular deterioration, nephropathy, retinopathy and neuropathy (7-9). In addition, it has been demonstrated that AG inhibits the formation of AGEs by interacting with and quenching dicarbonyl compounds (10), protecting against myocardial contractile dysfunction (11). Thus, elucidating and dissecting the involvement of AG in diabetes-associated cardiac fibrosis could be useful in preventing or treating ROS- and AGE-related pathologies on the verge of an epidemic such as T2DM. Our aim was to investigate whether AG supplementation may reduce cardiac fibrosis and the gene expression profile of oxidative stress in diabetes-associated cardiac fibrosis.

Materials and methods

Sources of antibodies and qPCR primers. The sources of commercially available antibodies can be found in Table SI. The collagen type I antibody (1/5,000) was generated and provided by Dr Schuppan (University of Mainz, Mainz, Germany) (12,13). The qPCR primers used are shown in Table SII.

Cell culture and treatments. Cell culture experiments were performed in primary rat myofibroblasts at high glucose (>17.5 mM, considering glucose concentration in culture medium) and high insulin concentrations, induced hyperglycemia/hyperinsulinemia conditions similar to diabetes (14,15). Primary heart cultures were obtained from neonatal rats, and myofibroblasts were isolated according to Boateng *et al* (16). Three days after cell isolation, rat myofibroblasts were seeded on six-well plates (300,000 cells/well) in DMEM/F12 supplemented with 10% FBS, 0-50 nM insulin (4512-01 CellPrime® r Insulin; EMD Millipore Corporation), 0-17.5 mM glucose (Thermo Fisher Scientific, Inc.), fungizone, penicillin and streptomycin for 48 h. The medium was replaced with serum-free medium before treatment with 0-1 mM AG (Acros Organics). The untreated cells were maintained in DMEM/F-12 supplemented with 10% FBS. According to the manufacturer's description, DMEM/F-12 medium contains 3.15 g/l (17.5 mM) of glucose, plus traces of glucose originating from the serum. Concentrations of glucose above 10 mM are analogous to a diabetic condition within the cell culture system (17).

Time-course (15 min to 24 h) and dose-response (0.5-1.0 mM) experiments were carried out to determine the final concentration of AG and the best time-point for collagen type I induction (24 h). In some experiments, either 0.12 μM (5 μg/ml) of rat RAGE-neutralizing antibody (AF1616-SP) or normal goat IgG control (AB-108-C; R&D Systems) was added to the cells 1 h prior to incubation with AG, according to the recommended concentration for blockade of receptor-ligand interaction from the manufacturer. The optimal concentration for collagen type I induction was determined experimentally.

Animals. This study was carried out on 45 male Wistar rats with weights ranging between 100 and 150 g. Rats were anesthetized with ketamine/xylazine (i.p. 100 mg/kg and 10 mg/kg b.w.) followed by a lethal 3x anesthesia dose, according to The Guidelines of The American Veterinary Medical Association. Confirmation of death was performed by observation of cardiac arrest for 10 min or longer. This was variable among animals until lack of pulse, breathing and response to firm toe pinch was observed. The verification of death was supplemented by rigor mortis verification. Rats were obtained from the animal facility of the University Center of Health Science (CUCS), Guadalajara University. All animal studies and humane endpoints set out for this study were in accordance with the rules of Ethical and Technical Specifications for Care and Management outlined in The National Institutes of Health's Guide, and approved by Jalisco State Agency for the Care and Use of Laboratory Animals (approval no. 16/UG-JAL/2008). During the study, the animals were kept in polypropylene cages with *ad libitum* access to water in order to gain weight until reaching 200-250 g, when their fasting blood glucose levels were monitored prior to diabetic induction.

Induction of experimental diabetes in rats. Rats were fed for diabetic induction with an HFCD composed of 20% sucrose, 10% coconut oil and 1% cholesterol per kilogram for 2 weeks. Two-thirds of the rats fed with HFCD (n=30) received daily intraperitoneal injections of freshly prepared solution with 20 mg/kg of STZ (Sigma-Aldrich Co.) dissolved in 0.1 M sodium citrate buffer (pH 4.5) during the following 5 days, while age-matched controls received buffer-only injections and HFCD diet. On the first day after injection, the fasting blood glucose was measured from rat tail-veins by using a blood glucometer. Rats with fasting blood glucose levels >200 mg/dl were deemed diabetic. One-third (n=15) of the animals continued to be fed with HFCD diet (control group).

Groups and treatment. The rats not receiving diabetic induction were used as negative controls (non-diabetic group). The diabetic rats were randomly allotted to non-treated diabetic (HFCD+STZ) and diabetic-treated (HFCD+STZ+AG) groups (n=15 rats/group). The HFCD+STZ+AG group was treated with daily intraperitoneal administration of AG (20 mg/kg) throughout the experiment (Fig. 1). Methodologically, a third control group without diabetes but with AG treatment was not included since two control groups, negative control (HFCD-fed) and positive control (STZ-injected), were already used in the study (18,19). At 15, 20 and 25 weeks after treatment, all animals were sacrificed prior to blood extraction. Blood was taken directly from the cardiac chamber and the heart

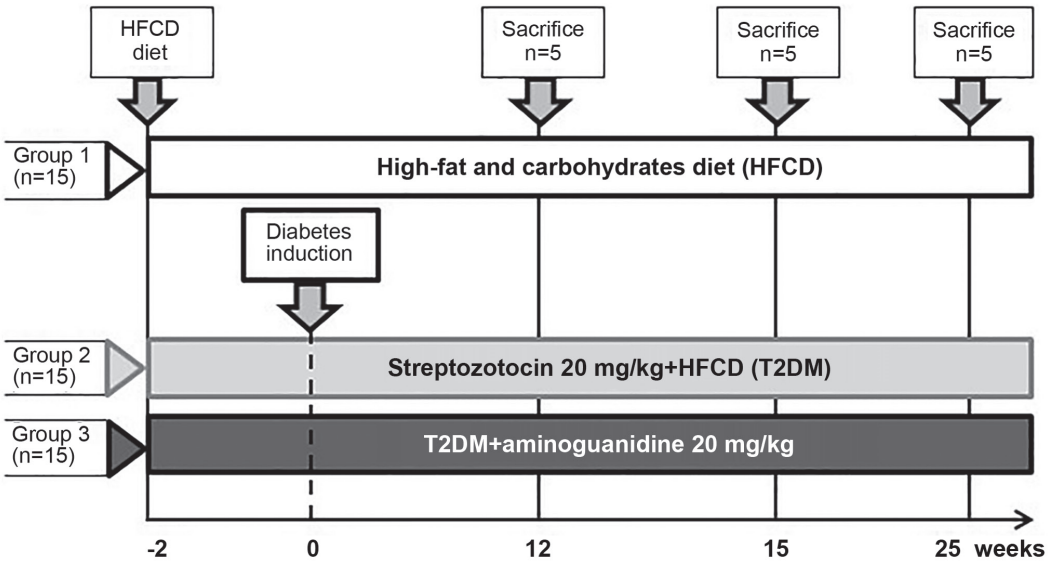

Figure 1. Study design. Male Wistar rats were fed ad libitum with a HFCD for 2 weeks before induction of T2DM. Control rats (n=15) were fed with HFCD throughout the experiment and did not receive STZ (Group 1). Rats were rendered diabetic with multiple low doses of STZ (20 mg/kg/day for 5 days) (Groups 2 and 3). The third group of rats (n=15) was treated with AG (20 mg/kg/day). All groups of rats (n=5/group) were sacrificed, at 12, 15, and 25 weeks post T2DM induction. HFCD, high-fat, high-carbohydrate diet; T2DM, type 2 diabetes mellitus; STZ, streptozotocin.

was removed for molecular and histological analysis. Blood samples were collected and stored at -80˚C, and myocardial tissue samples were collected and subsequently formalin-fixed for further analysis.

Histological analysis. Hearts were excised, washed with saline solution and placed in 10% formalin. Then, they were cut transversely, close to the apex, to visualize the left ventricle and right ventricle, and several sections of heart (5-μm thick) were prepared. Cardiac histology was assessed using hematoxylin and eosin (H&E) staining in paraffin-embedded sections using standard commercial methods. Fibrosis was assessed using both Masson's trichrome and Sirius red/Fast green staining in paraffin-embedded sections using established methodology (20). The cardiac histology was evaluated by a pathologist who was blinded from the experimental conditions. The number of microscopic fields with fibrosis was recorded, and five affected fields were photographed. Image analysis (n=5 rats/week) was performed using a digital microscope and AxioVision v.7 software.

Western blotting. Cells lysate samples were processed using sodium dodecyl sulfate polyacrylamide gel electrophoresis (SDS-PAGE) 5-10% gels and nitrocellulose membranes. Actin served as an endogenous control of protein expression. Membranes were incubated with the primary antibodies shown in Table SI and corresponding peroxidase-coupled secondary antibodies from EMD Millipore Corporation. Images were captured with an Amersham™ Imager 600, and results were analyzed using ImageQuant™TL analysis software v8.1 (GE Healthcare Bio-Sciences) after enhanced chemiluminescence using Pierce™ ECL substrate (Thermo Fisher Scientific, Inc.).

α-Smooth muscle actin immunohistochemistry. Immunohistochemical staining on paraffin-embedded heart tissue was performed for each experimental time-point using a primary antibody against αSMA (Millipore anti-alpha-actin (smooth muscle) clone E184, rabbit monoclonal; dilution: 1:500), followed by a secondary biotinylated anti-rabbit IgG, and developed using the Histostain® Plus detection system (Invitrogen; Thermo Fisher Scientific, Inc.).

cDNA synthesis and reverse transcription-quantitative PCR (qPCR). Total RNA was isolated from 100 mg of tissue using TRIzol reagent (Invitrogen; Thermo Fisher Scientific, Inc.), quantified by determination at OD_{260} and stored at -80˚C. Two micrograms of total RNA was reversed-transcribed using an oligo(dT) primer and M-MLV reverse transcriptase (Invitrogen; Thermo Fisher Scientific, Inc.) according to the manufacturer's protocol. The cDNA generated was stored at -20˚C.

Real-time PCR was developed with diluted cDNAs using pre-developed and validated TaqMan® gene expression assays by Applied Biosystems; Thermo Fisher Scientific, Inc.: *Nos2* ID: Rn02132634_s1; *Nox4* ID: Rn00585380_m1; *Col1a1* ID: Rn01463848_m1; *Ucp2* ID: Rn01754856_m1; *Nrf2* ID: Rn00477784_m1; *β-actin* ID: Rn00667869_m1, according to the manufacturer's protocol. The *β-actin* qPCR gene efficiency had been validated previously. Amplification by real-time PCR was performed on the StepOne™ Real-Time PCR System (Applied Biosystems; Thermo Fisher Scientific, Inc.). Each qPCR analysis included duplicate wells, and appropriate control reactions were performed for all samples. The expression level of each gene of interest was calculated using the $2^{-\Delta\Delta Cq}$ method (21). Gene amplification was normalized against *β-actin* expression in each sample, and gene expression levels are shown as relative expression units by comparing them to the control group as an internal calibrator.

Total RNA from cultured primary rat myofibroblasts was isolated using TRIzol® (Invitrogen; Thermo Fisher

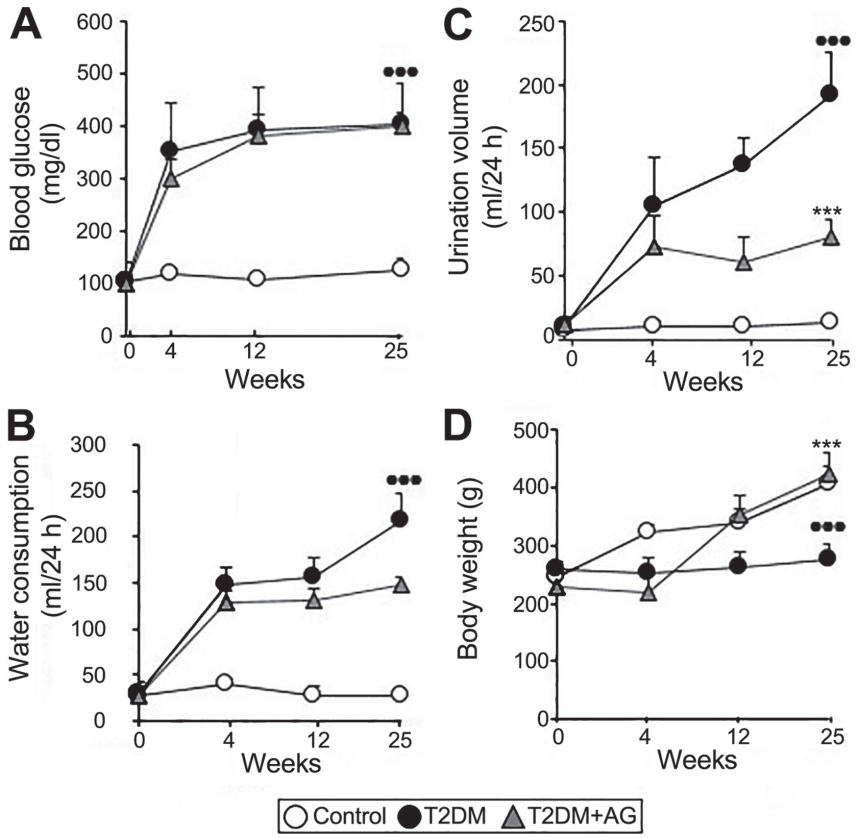

Figure 2. T2DM rats show increased blood glucose, urinary volume and water consumption with modest body weight gain. Rats treated with high-fat, high-carbohydrate diet plus low-dose streptozotocin injection (T2DM) developed (A) hyperglycemia, accompanied by increased (B) water consumption, (C) urination volume and (D) modest body weight gain. T2DM+AG did not change blood glucose concentration or water consumption, but urinary volume and body weight were improved. Results are expressed as the mean ± SD. n=5/group. •••P<0.001 vs. control; ***P<0.001 vs. T2DM. T2DM, type 2 diabetes mellitus; AG, aminoguanidine.

Scientific, Inc.). Total RNA was reverse-transcribed using an Ecodry® Premix Kit (Clontech), and qPCR was performed in a Roche Light Cycler 480 with FastStart SYBR-Green Master (Roche Diagnostics). Expression of the target gene was calculated by the cycle-threshold method, and results are expressed as the relative fold-change with respect to the appropriate control group. Values were normalized to the housekeeping gene *β-actin*. Each qPCR reaction was run in triplicate.

Statistical analysis. Data are expressed as mean ± standard deviation of the mean (SD). Statistical comparisons within groups were performed by two-way ANOVA followed by Tukey's multiple comparison test. Gene expression comparisons were performed by Kruskal-Wallis test followed by Mann-Whitney U test post hoc test. Data are shown in all figures, and P<0.05 was used to indicate a statistically significant difference.

Results

T2DM rats show increased blood glucose, urinary volume and water consumption with modest body weight gain. To begin our experimental investigations, we confirmed that our T2DM model shows representative symptoms of human T2DM such as hyperglycemia, polydipsia and polyuria. The HFCD, concomitantly with STZ, induced insulin resistance resulting in hyperglycemia maintained throughout the study (Fig. 2A). This was accompanied by increased water consumption (Fig. 2B) and urinary volume (Fig. 2C) as well as modest body weight gain (Fig. 2D). Partial but not full pancreatic islet β-cell destruction-a central feature in T2DM (22) -was observed in induced-T2DM rats (Fig. S1). Importantly, AG had no hypoglycemic effect as shown by unchanged fasting blood sugar concentration and water consumption but improved urinary volume and weight in AG-treated diabetic rats.

AG-treated rats showed improvement of myocardial architecture compared to non-treated diabetic rats. To analyze the prevention of diabetes-associated cardiovascular damage by AG, rats were sacrificed in weeks 12, 15 and 25, and their cardiac tissues were subjected to histological analysis. After 15 weeks, T2DM rats already had irregular myofibrillar orientation as shown by H&E staining (Fig. 3E and H). By contrast, AG-treated diabetic rats showed improvement of myocardial architecture compared to non-treated diabetic rats (Fig. 3F and I).

AG-treated rats exhibit less fibrosis and α-smooth muscle actin (αSMA) protein expression than T2DM rats. To further evaluate the potential antifibrotic role of AG *in vivo*, hearts were processed for Sirius red/Fast green, Masson's trichrome staining and αSMA immunohistochemistry (IHC). We observed progressive interstitial myocardial fibrosis in T2DM rats by 12 weeks after induction (Fig. 4A-e and A-h) while AG-treated

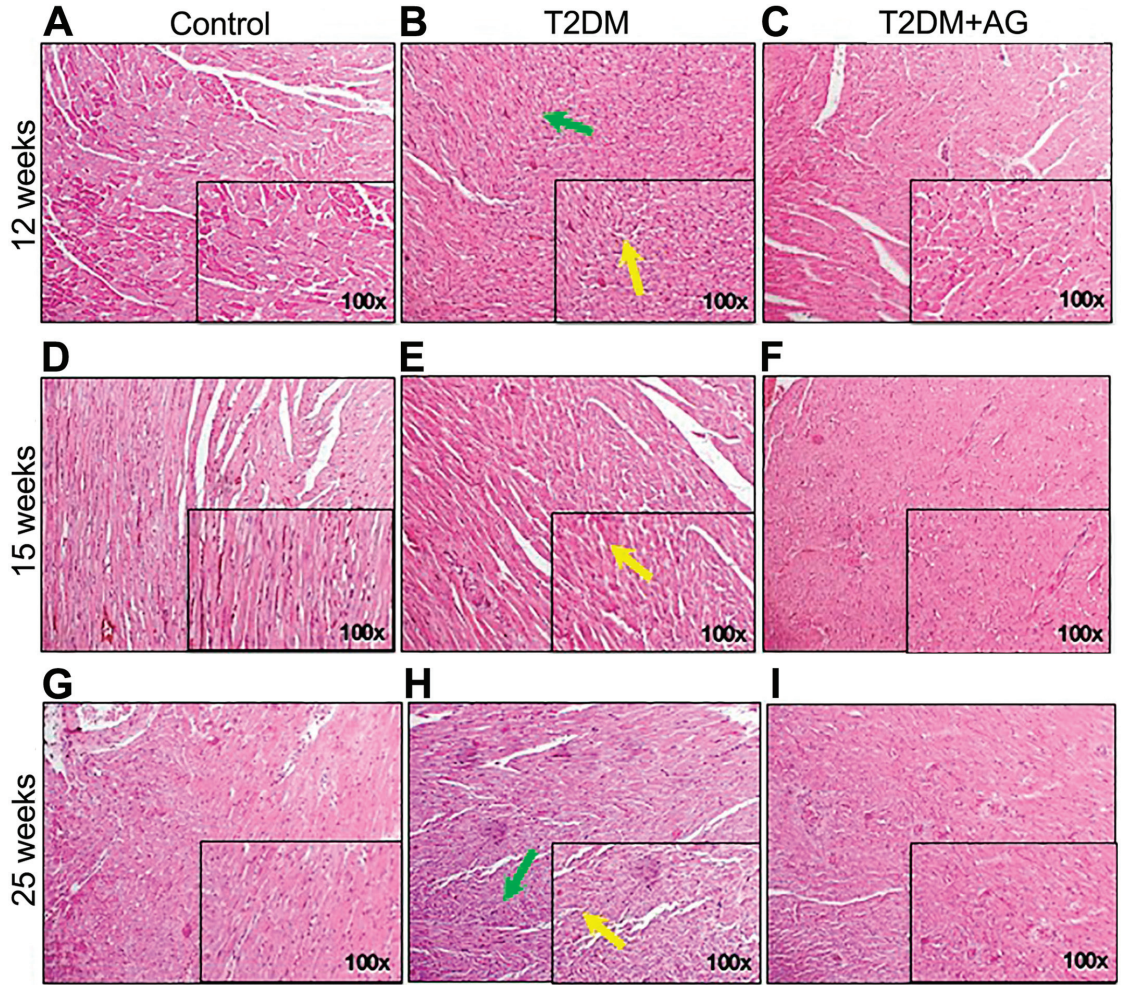

Figure 3. AG-treated rats showed improvement of myocardial architecture compared to non-treated diabetic rats. Hematoxylin-eosin staining revealed less myocardial damage in T2DM+AG rats; original magnification, x10. Green arrows indicate morphological derangement of the injured tissue architecture. Yellow arrows myofibrillar disorientation and cardiomyocyte disorganization. These changes were observed to a lower extent in the hearts from AG-treated diabetic animals. (A, D and G) Control group; (B, E and H) T2DM group; (C, F and I) T2DM+AG group. T2DM, type 2 diabetes mellitus; AG, aminoguanidine.

diabetic rats exhibited less fibrosis (Fig. 4A-f and A-i). Likewise, Sirius red/Fast green quantification (Fig. 4B) and Masson's trichrome staining (Fig. 5A) revealed less fibrosis compared to the T2DM group. Consistently, AG significantly downregulated *Col1a1* mRNA expression 8.3-fold at week 12, although no changes were observed at week 25 in T2DM+AG compared to T2DM rats (Fig. 5B).

Considering the expression of αSMA in myofibroblasts as a marker in fibrosis (23), we next studied the role of AG in αSMA protein expression. AG-treated rats exhibited less αSMA expression (Fig. 6A-f and A-i) compared to non-treated T2DM rats (Fig. 6A-e and A-h). Likewise, αSMA IHC quantification showed lower αSMA expression in T2DM+AG compared to T2DM rats (Fig. 6B).

Collectively, these results suggest that AG has an important antifibrotic role in T2DM rats by reducing fibrosis deposition and αSMA induction in diabetes-associated cardiac fibrosis.

AG treatment downregulates oxidation-associated gene expression in cardiac tissue. Since oxidant stress-sensitive proteins are known to regulate cardiac collagen type I (24), we looked into the mRNA profile of oxidant and antioxidant genes in rats and in primary myofibroblasts treated with AG. We found that *Nos2* (endothelial nitric oxide synthase) and *Nox4* (NADPH oxidase 4) mRNA expression was upregulated in diabetic rats. By contrast, AG-treated rats had less *Nos2* and *Nox4* mRNA expression in cardiac tissue, in a time-dependent manner (Fig. 7A). Likewise, *Nrf2* (nuclear factor (erythroid-derived 2)-like 2) and *Ucp2* (uncoupling protein 2) mRNAs, well-known antioxidant-associated genes capable of modulating ROS (25,26), were upregulated under oxidative conditions in T2DM rats and reduced upon AG treatment (Fig. 7B).

Taken together, these results suggest an antioxidant effect of AG in diabetic-associated cardiac fibrosis.

AG reduces oxidation-associated collagen type I expression through ERK1/2 and SMAD2/3 signaling in myofibroblasts. Considering that AG has ROS-detoxification activity (27-29), and that ROS lead to ECM accumulation in diabetes (30), we investigated the role of AG in AGE signaling in primary myofibroblasts. Primary myofibroblasts from neonatal rats were exposed for 48 h to extended high insulin (0-50 nM) and high glucose (0-17.5 mM) levels to induce the impairment of insulin signaling and to desensitize glucose transport (HIG

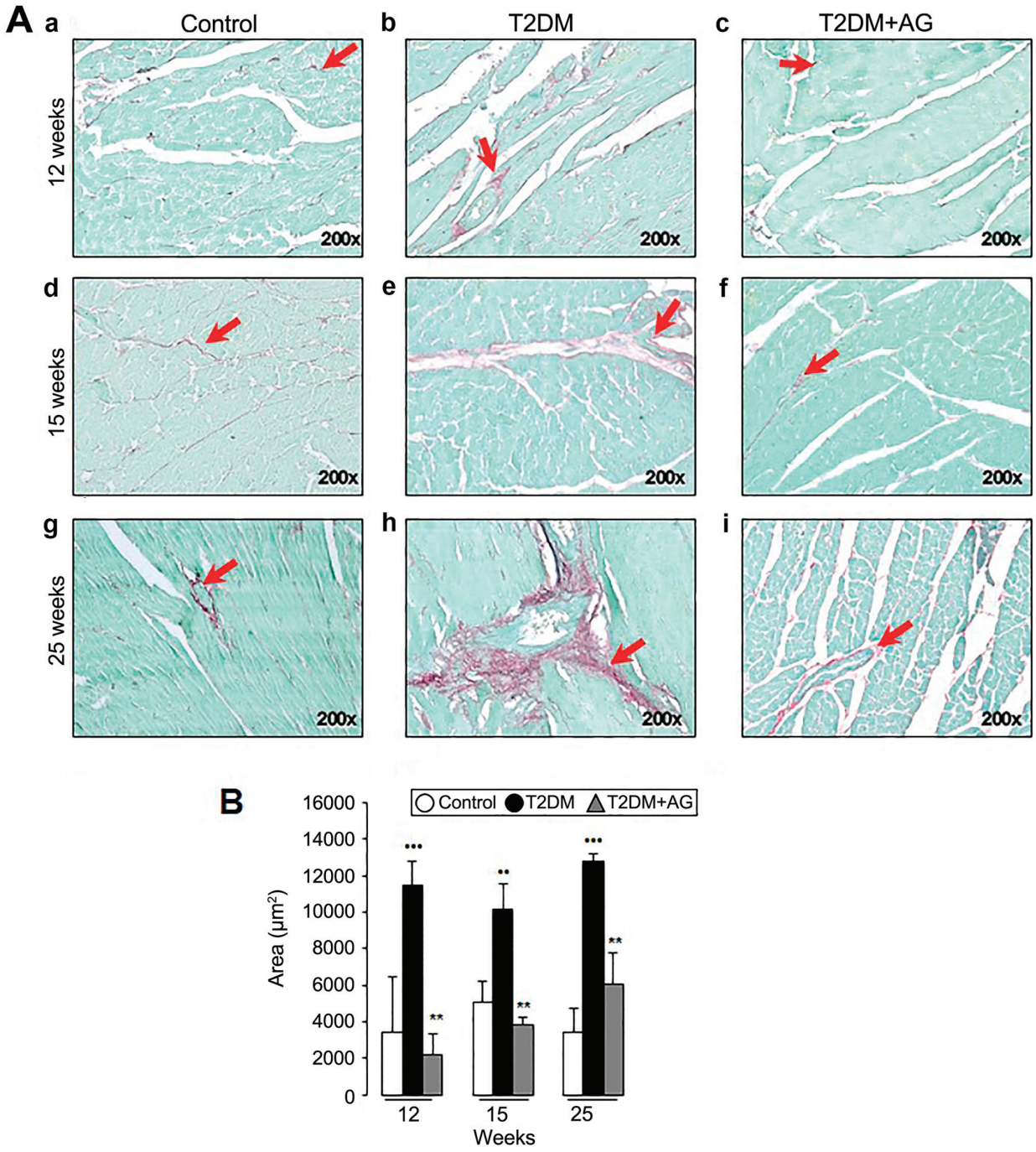

Figure 4. AG-treated rats exhibit less Sirius red staining compared with T2DM rats. (A) Sirius red/Fast green staining for collagenous proteins revealed extensive fibrosis in T2DM. (a,d and g) Control group; (b, e and h) T2DM group; (c, f and i) T2DM+AG group. Red arrows show the gradual development of interstitial fibrosis at different durations after diabetes induction (red stained area). (B) Sirius red/Fast green staining quantification, expressed as a positive area. Results are presented as the mean ± SD. n=5/group. "P<0.01, ""P<0.001 vs. control; **P<0.01 vs. T2DM. T2DM, type 2 diabetes mellitus; AG, aminoguanidine; w, weeks; αSMA, α-smooth muscle actin.

conditions) (31). Cells were further treated with AG (0-1 mM) for 24 h to analyze the effect of AG on the activation of kinase(s), such as the JAK/STAT pathway (32), the MEK1/2 pathway (33,34), SMAD2/3 (35) and AKT signaling (36), implicated in oxidative-associated fibrogenesis.

AG reduced phosphorylation of ERK1/2 and SMAD2/3 but not AKT1/2/3^{473}Ser, AKT1/2/3^{308}Thr or STAT3^{705}Tyr in primary rat myofibroblasts (Fig. 8A). Moreover, we looked into oxidant stress-sensitive pro-inflammatory mediators such as interleukin-6 (IL-6), and tumor necrosis factor α (TNFα), known to regulate collagen type I expression, and observed similar *Tnfα* aSnd *Il6* mRNA expression in AG-treated compared to untreated myofibroblasts in diabetic conditional medium (Fig. 8B). Similarly, no changes in *Nos2*, *Nox4* and *Ucp2* mRNA expression were observed in AG-treated compared to untreated myofibroblasts (Fig. S2).

Based on the *in vivo* findings, and because collagen is one of the main targets of reducing sugars and dicarbonyl compounds in diabetes (37,38), we further investigated the effect of AG on collagen type I expression in primary rat

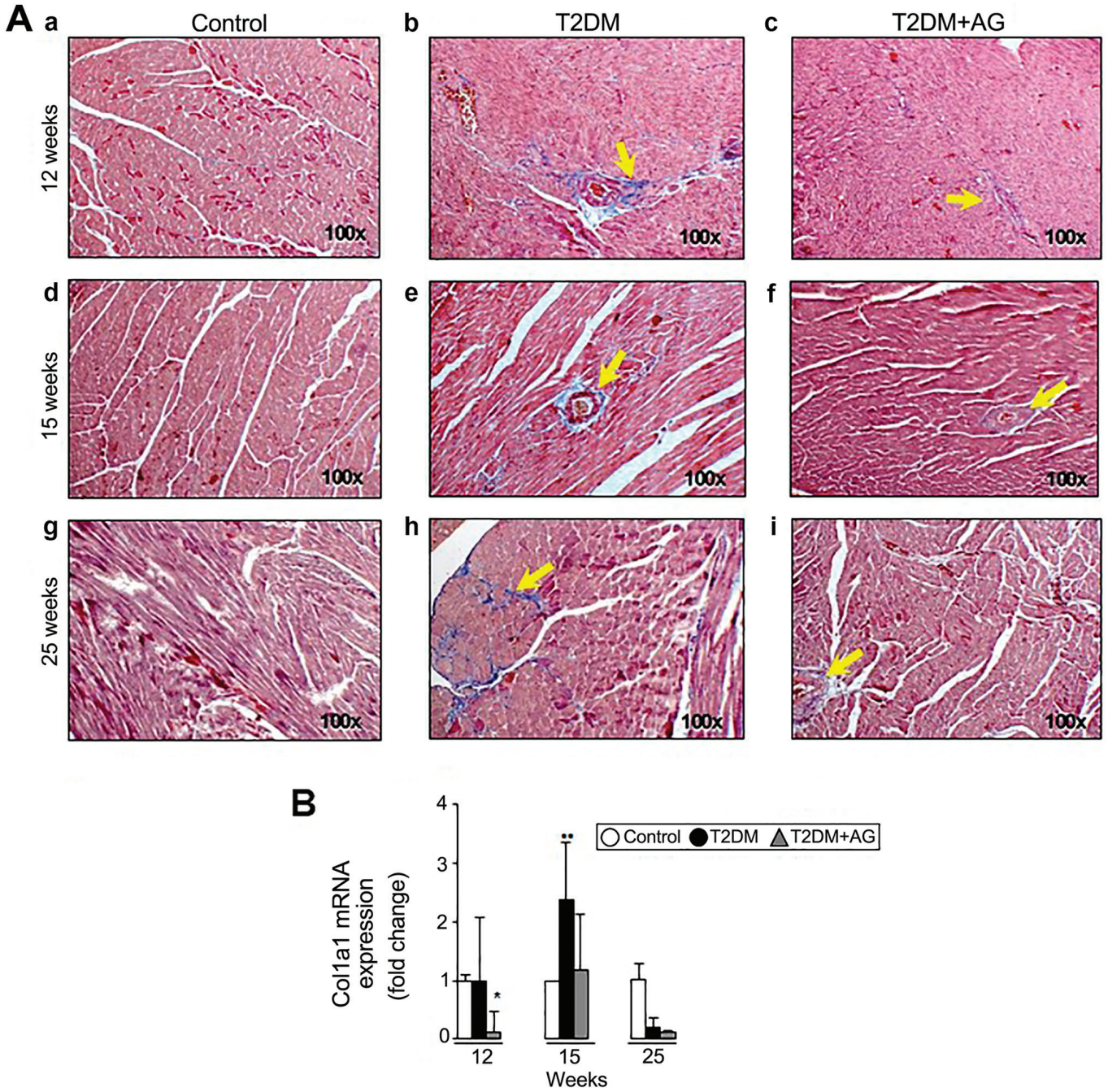

Figure 5. AG-treated rats exhibit less cardiac fibrosis compared to T2DM rats. (A) Masson's trichrome staining shows that AG-treated rats had reduced fibrosis deposition compared to untreated T2DM rats. (a,d and g) Control group; (b, e and h) T2DM group; (c, f and i) T2DM+AG group. Yellow arrows show collagen fibers; original magnification, x10. (B) Cardiac Col1a1 mRNA expression. Gene amplification was normalized against β-actin expression, and gene expression levels are shown as fold-changes. Results are expressed as the mean ± SD. n=5/group. **P<0.01 vs. control; *P<0.05 vs. T2DM. T2DM, type 2 diabetes mellitus; AG, aminoguanidine; Col1a1, collagen type 1 α 1.

myofibroblasts. Intra- and extracellular collagen type I protein expression (Fig. 8C) and *Pdgfb*, *Tgfβ1* and *Col1a1* mRNA expression (Fig. 8D) were downregulated in AG-treated compared to untreated myofibroblasts in diabetic conditional medium. Therefore, our results indicate that AG reduces collagen type I deposition in myofibroblasts through convergent ROS-sensitive ERK1/2 and SMAD2/3 signaling.

AG reduces collagen type I expression via RAGE in myofibroblasts. Since *Ager* mRNA was significantly after HIG conditions (Fig. 9A), the effect of AG and the importance of RAGE for collagen type I expression were explored using an antibody blockade strategy. Treatment with a RAGE-neutralizing antibody before AG treatment resulted in a significant decrease of total collagen type I expression in myofibroblasts (Fig. 9B), suggesting that AGE/RAGE activation is requisite for increased collagen type I expression in myofibroblasts (Fig. 10).

Discussion

Until now, many kinds of animal models have been used for diabetes research, but neither surgical nor chemical models

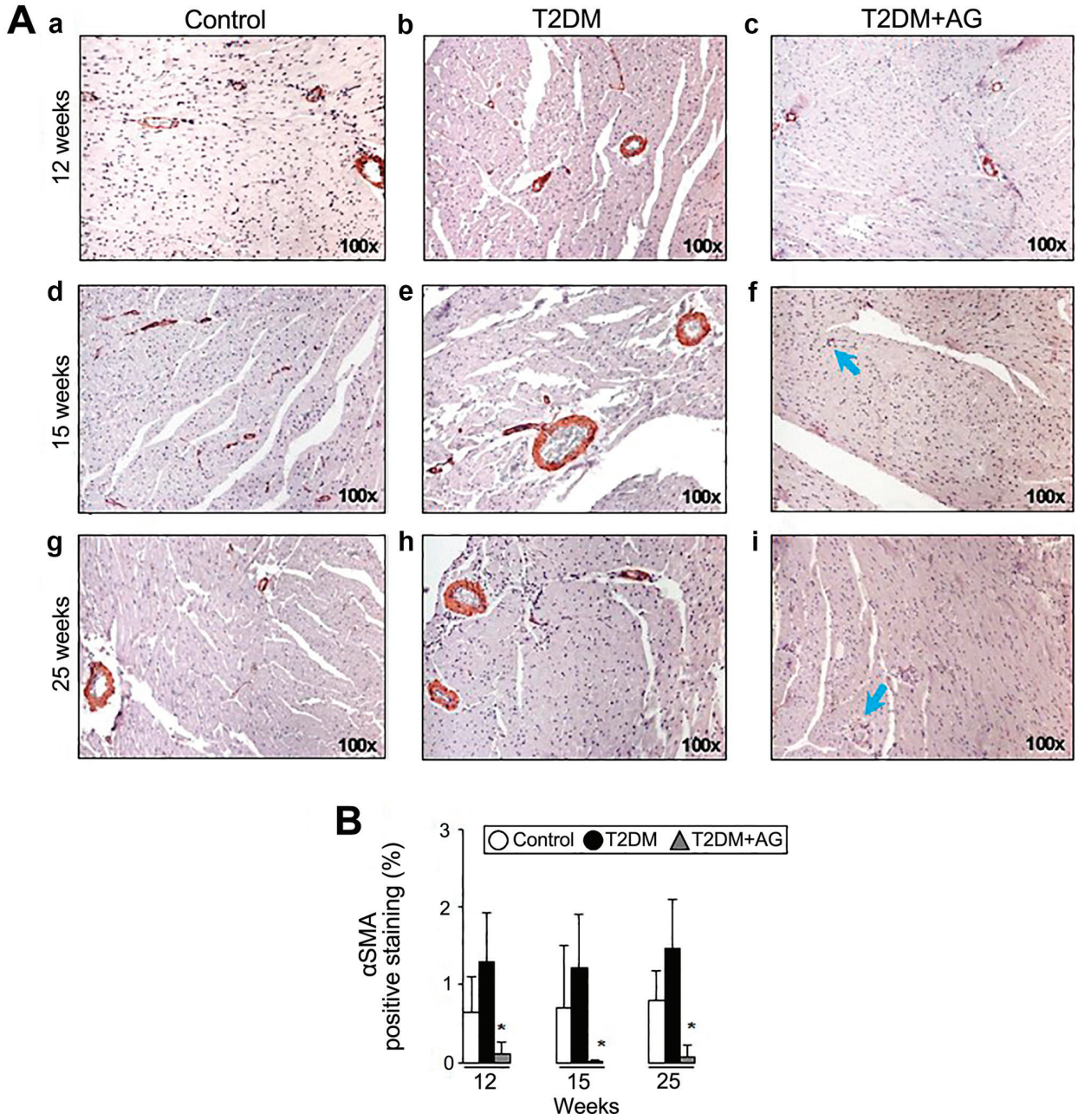

Figure 6. AG-treated rats exhibit less αSMA protein expression compared with T2DM rats. (A) αSMA immunohistochemical representative micrographs and (B) quantification show a significant reduction of αSMA-positive staining in T2DM+AG rats. (A) (a, d and g) Control group; (b, e and h) T2DM group; (c, f and i) T2DM+AG group. Blue arrows indicate less expression of αSMA in T2DM+AG rats compared with T2DM rats. Results are expressed as the mean ± SD. n=5/group. *P<0.05 vs. T2DM. αSMA, α-smooth muscle actin; T2DM, type 2 diabetes mellitus; AG, aminoguanidine.

simulate human T2DM (3,39-42). STZ induces cardiac fibrosis, contractile dysregulation and mitochondrial damage (43), all AGE-related disorders (44). In fact, lower doses of STZ (≤50 mg/kg) in conjunction with a diet rich in fat (40% of total dietary kcal) have been successfully employed to induce T2DM (44,45). In the present study, we reduced the dose of STZ to 20 mg/kg (46), and extended the time reported from 18 weeks to 25 weeks (47), to replicate chronic features of T2DM and evoke cardiac fibrosis.

In our model, diabetic rats showed slight weight gain, polydipsia and polyuria without tendency to cause ketosis and without gradual recovery to normoglycemia. In addition, the use of insulin therapy to sustain life was not necessary, suggesting that STZ doses plus HFCD only reduced the pancreatic β cell mass, but did not eliminate them. Importantly, a symptom for the onset of T2DM is a sudden loss of weight due to frequent urination and high blood glucose that is no longer being taken up, and when some form of treatment is applied to allow the uptake of glucose, patients often see an increase in body weight (45). This was indeed observed in the STZ-induced diabetic rats, indicating the presence of T2DM. However, insulin resistance and its associated multiorgan dysfunction assessment were not performed, which might be a limitation of this study.

Recent investigations on diabetes have demonstrated that impaired mechanisms dependent on UCP2 (46),

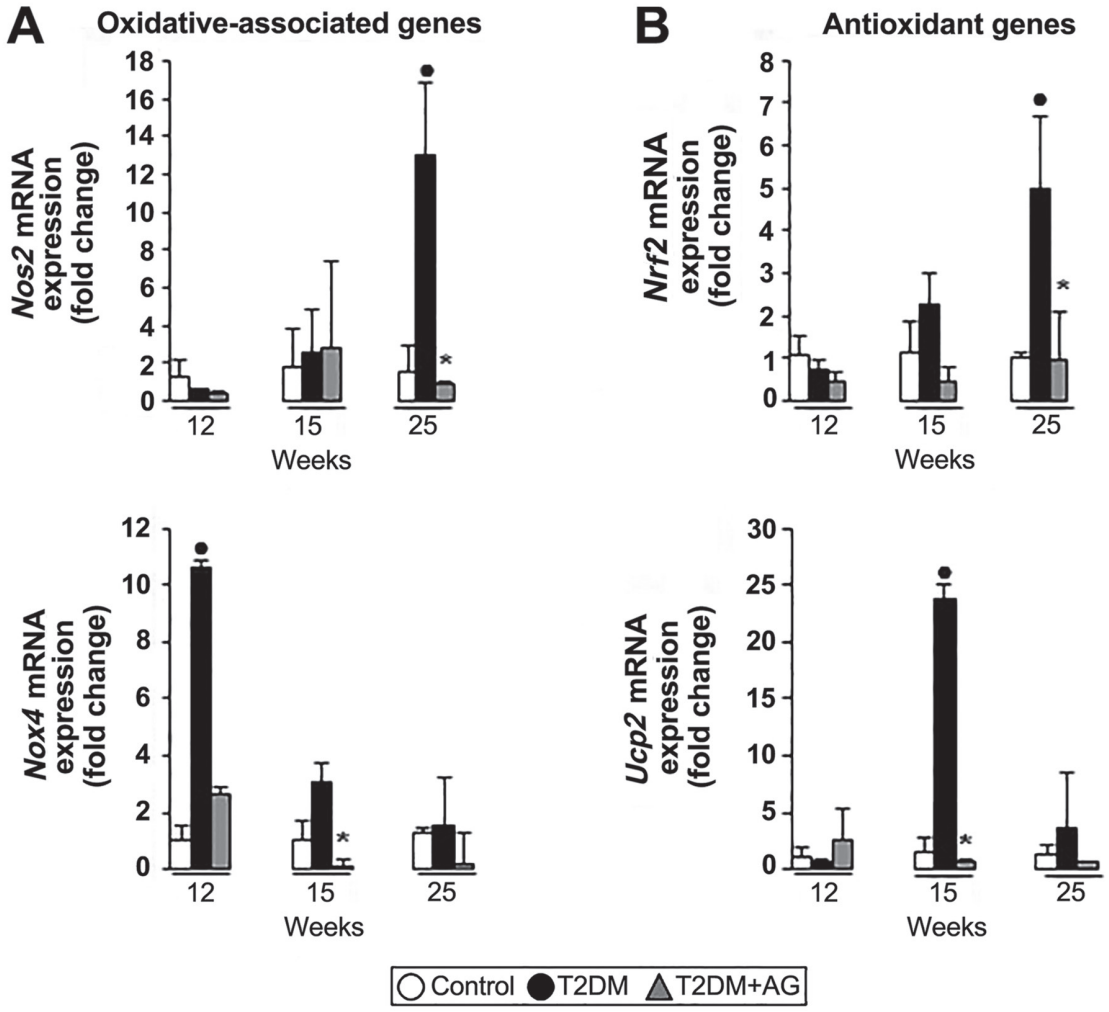

Figure 7. AG treatment downregulates oxidation-associated gene expression in cardiac tissue. (A) AG treatment downregulates the expression of oxidative-associated Nos2 and Nox4 mRNAs, and (B) antioxidant Nrf2 and Ucp2 mRNA expression is upregulated in cardiac tissue of T2DM rats. Gene amplification was normalized against β-actin expression, and gene expression levels are shown as fold-changes. The values represent the mean ± SD. n=5/group. •P<0.05 vs. control; *P<0.05 vs. T2DM. T2DM, type 2 diabetes mellitus; AG, aminoguanidine; w, weeks; Nox4, NADPH oxidase 4; NO, nitric oxide; Nrf2, nuclear factor (erythroid-derived 2)-like 2; Ucp2, uncoupling protein 2.

Nrf2 (47,48), Nox4 (49-52) and endothelial nitric oxide synthase (eNOS) (53-55) participate in collagen type I deposition, therefore reducing myocardial compliance (56,57). However, it is still unclear how these molecular signals participate in the diabetes-associated fibrogenic response.

For this reason, we used AG as a therapeutic agent for cardiac fibrosis associated with T2DM. AG is a water-soluble molecule that scavenges toxic 1,2-dicarbonyl compounds such as methylglyoxal, and attenuates oxidative stress by inhibiting the formation of AGEs and nitric oxide synthase (58).

The treatment with AG reduced cardiac *Nox4* and *Nos2* mRNA expression compared to untreated diabetic rats. By contrast, the unchanged *Nos2*, *Nox4* and *Ucp2* mRNA expression in primary myofibroblasts but not in the diabetic rats suggests a dual effect of AG in the diabetic heart: Antioxidant in non-myofibroblasts, and antifibrotic in myofibroblasts. This is supported by the downregulation of collagen type I protein, *Pdgfb*, *Tgfβ1* and *Col1a1* mRNA expression and ERK1/2-SMAD2/3 signaling in AG-treated myofibroblasts. It is also possible that AG *in vivo* has a positive effect on renal AGE-associated damage (59,60), since AG treatment improved urinary output. This effect may not be related to changes in blood pressure but to reduction of AGE-mediated tubulointerstitial injury and endothelium-dependent relaxation (61). Nevertheless, more *in vivo* studies are needed to dissect the organ-specific molecular signals activated by AG in diabetes-associated fibrosis.

In vitro, hyperglycemia is involved in the activation of cardiac fibroblasts, promoting a fibrogenic phenotype and release of cytokines and growth factors with potential to generate ROS (62-64); however, the significance of these findings *in vivo* is unclear, and robust evidence is required to demonstrate that diabetes-associated myocardial fibrosis is due to hyperglycemia. Although some metabolic conditions that occur in diabetes cannot be resembled *in vitro*, myofibroblasts were cultured in hyperglycemic medium, with and without insulin, to analyze the AG effect in the diabetic niche (65,66).

The appearance of hyperglycemia in T2DM is preceded by a phase of hyperinsulinemia, which is able to overcome tissue resistance and transport glucose into cells. This is followed by a stage of hyperglycemia that may overlap with

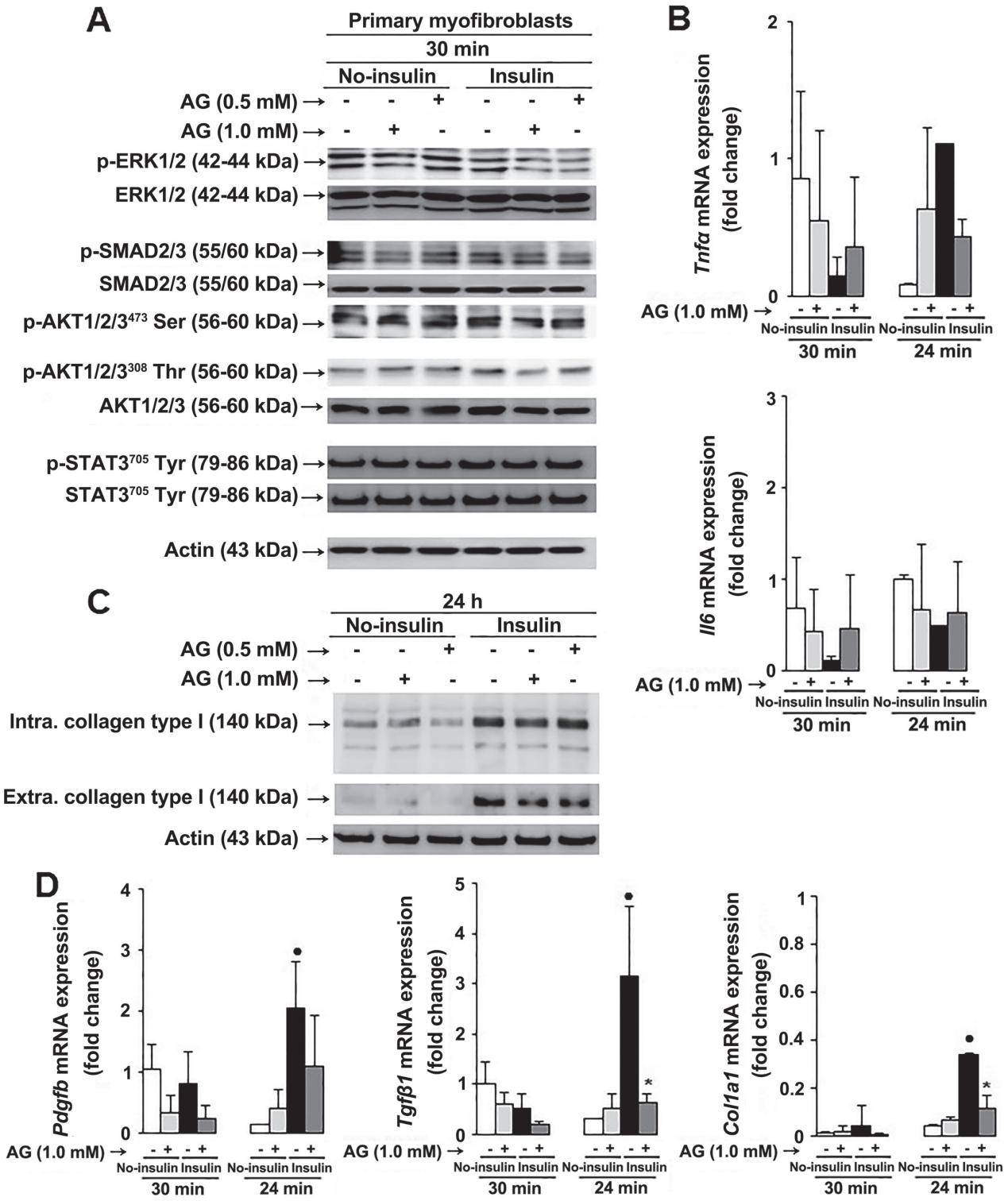

Figure 8. AG reduces collagen type I deposition through ERK1/2-SMAD2/3 signaling in myofibroblasts. Primary myofibroblasts were preincubated with 0-50 nM insulin and 0-17.5 mM glucose for 48 h and treated with and without 0-1 mM AG up to 24 h. Western blot analysis shows reduced ERK1/2 and SMAD2/3 but not AKT1/2/3 and STAT3 phosphorylation in AG-treated compared to untreated myofibroblasts. (A) Values were corrected by the level of actin protein expression and are expressed as fold-changes vs. controls. (B) Similar Tnfα and Il6 mRNA expression in AG-treated compared to untreated myofibroblasts. (C) AG downregulates intra- and extracellular collagen type I protein expression and (D) Pdgfb, Tgfβ1 and Col1a1 mRNA expression in AG-treated compared to untreated myofibroblasts in diabetic conditional medium. Total collagen type I values were calculated as intracellular collagen type I/actin plus extracellular collagen type I/actin ratios. Gene amplification was normalized against β-actin expression, and gene expression levels are shown as fold-changes. The values represented the mean ± SD. n=5/group. •P<0.05 vs. no-insulin control at 24 h; *P<0.05 vs. untreated diabetic conditional medium at 24 h. AG, aminoguanidine; *Col1a1*, collagen type 1 α 1; *IL-6*, interleukin-6; MAPK, mitogen-activated protein kinase; *Pdgfb1*, platelet-derived growth factor β1; signal transducer and activator of transcription 3 (STAT3); *Tgfβ1*, transforming growth factor β1; *Tnfα*, tumor necrosis factor α.

hyperinsulinemia for some time. Thus, experimental conditions of high glucose and high glucose plus high insulin were designed to recapitulate T2DM (15,67), and to induce insulin resistance in myofibroblasts. Thus, AKT signaling

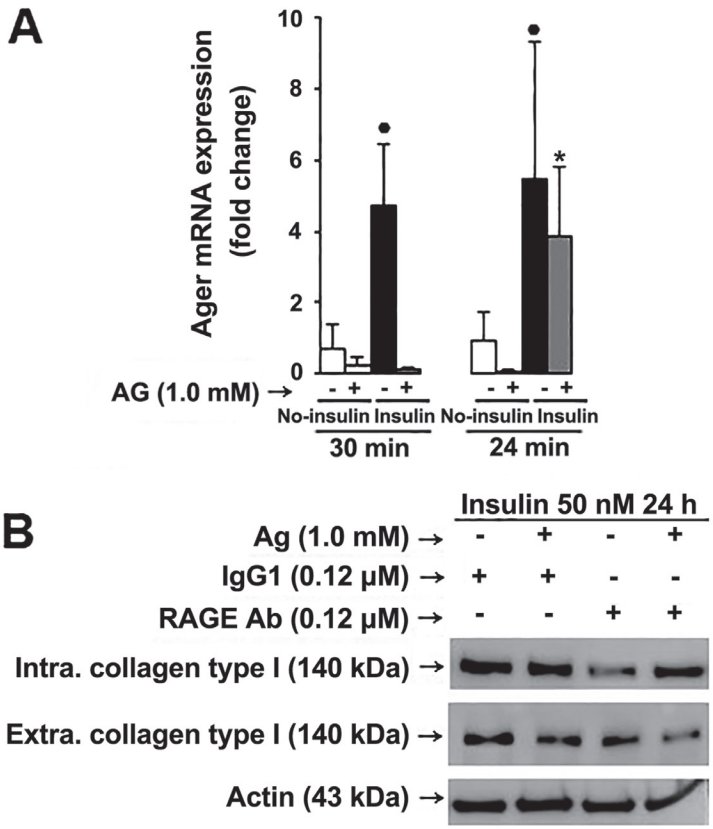

Figure 9. AG reduces collagen type I deposition via RAGE in myofibroblasts. Ager mRNA expression was analyzed by reverse transcription-quantitative PCR in primary myofibroblasts preincubated for 1 h with a RAGE-neutralizing Ab and treated with 0-1 mM AG for 24 h. (A) mRNA expression was normalized against actin expression and expressed as fold-change compared to cells treated with the corresponding IgG_1 isotope control. (B) Total collagen type I was lowered by the RAGE-neutralizing Ab upon treatment with AG. Values were calculated as intracellular collagen type I/actin plus extracellular collagen type I/actin ratios. Results from the western blot analysis were corrected by the level of actin protein expression and are expressed as fold-changes compared with the controls which were assigned a value of 1, and are presented as the mean ± SD. n=2/group in experiments performed in triplicate. *P<0.05 vs. no-insulin control; *P<0.05 vs. untreated diabetic conditional medium at 24 h. Ab, antibody; AG, aminoguanidine; *Ager*, receptor for advanced glycation end products; RAGE, receptor for advanced glycation end products.

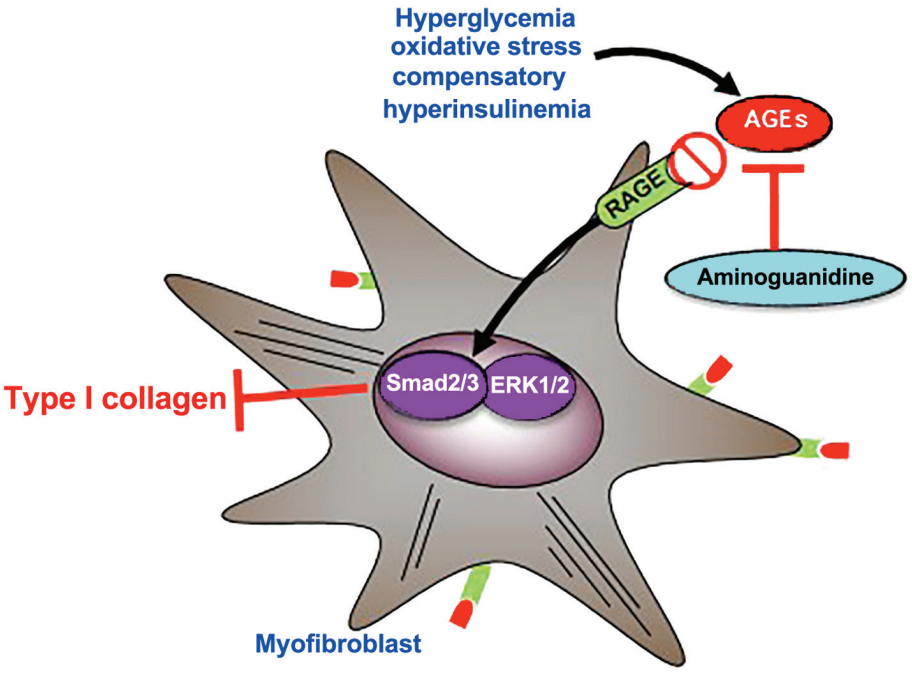

Figure 10. AG reduces collagen type I deposition via RAGE in myofibroblasts. Hyperglycemia, oxidative stress, insulin resistance, and compensatory hyperinsulinemia induce formation of AGEs that can be inhibited by AG in diabetes-induced cardiac fibrosis. AG reduces diabetes associated cardiac fibrosis by reducing pERK1/2, pSMAD2/3 and collagen type I expression likely through AGE/RAGE signaling. AG, aminoguanidine; RAGE, receptor for advanced glycation end products; AGEs, advanced glycation end products; p, phosphorylated; MAPK, mitogen-activated protein kinase.

was upregulated because insulin conveys its metabolic action through this pathway. However, western blot results suggested that AG, via AKT-independent signaling, reduces collagen type I likely through ERK1/2 and SMAD2/3 in myofibroblasts.

Importantly, the *in vitro* generation of final products of glycosylation was not performed, rendering an important limitation to the study. Nevertheless, the alteration of *Pdgfb*, *Tgfβ1* and *Col1a1* transcript levels and ERK1/2 and SMAD2/3 phosphorylation suggests the induction of diabetic conditions and a restoration of the pro-fibrotic program in myofibroblasts by AG.

Here, we propose that AG attenuates the fibrogenic response in T2DM rats, considering that AG reduces AGEs, advanced oxidation protein products (AOPP) (68), and inhibits iNOS activity (69,70), thus reducing oxidative-associated cardiac fibrosis. This was observed *in vivo* by αSMA IHC, Sirius red/Fast green and Masson's trichrome staining, and confirmed by the *in vitro* experiments on myofibroblasts. Therefore, our study provides strong support for the association between diabetes and myocardial fibrosis. Many studies have documented the underlying possible mechanism of AG in diabetes associated cardiac fibrosis, however, the effect of AG on collagen type I deposition through SMAD2/3-ERK1/2 via AGE/RAGE signaling represents the novelty of this study. These can be explained due to the glycation and AOPP-inhibiting properties of AG widely described in the scientific literature (68,71).

To provide further evidence for the contribution of SMAD2/3-ERK1/2 signaling, the use of specific MAP kinase inhibitors and/or siRNAs, might reverse the effects of AG-mediated cardioprotection. However, this was not assessed *in vitro*, which we acknowledge is another constraint to our research.

Since AG mitigates oxidative stress (72) and AGE levels (73) and reduces ROS formation (55,74), we analyzed oxidant and antioxidant-associated genes capable of modulating ROS, and oxidant stress-sensitive proteins known to regulate collagen type I expression. Our results suggest that AG reduces collagen type I expression and myofibroblast activation by either extenuating oxidative stress or by reducing the level of AGE-associated oxidative modifications such as RAGE binding (75). For instance, RAGE activation, depending on the cellular context and interacting ligand, can trigger different signaling pathways, which modulate oxidative stress that contributes to cellular dysfunction associated with diabetes (76). In this study, we demonstrated that AG exerts an antifibrotic effect likely through AGE/RAGE signaling, which is not associated to hypoglycemia. This is of special relevance since RAGE signaling contributes to oxidative stress-associated cardiac fibrosis (77).

In conclusion, STZ plus HFCD promotes T2DM and evokes pro-oxidative and pro-fibrotic responses attenuated in the presence of AG. Our results suggest that AG reduces oxidative-associated cardiac fibrosis by reducing the expression of pERK1/2, pSMAD2/3 and collagen type I, likely through AGE/RAGE signaling.

Acknowledgements

The authors would like to thank Dr Li Jieli (Department of Physiology and Biophysics, College of Medicine, University of Illinois) for her excellent assistance in the isolation of primary rat myofibroblasts.

Funding

This work was supported in part by PROINPEP 2014 (AR), awarded to support Ph.D. pharmacology program students, and by US Public Health Service (grant nos. R01 DK069286, R56 DK069286 and R56 DK069286-06S1) from the National Institute of Diabetes and Digestive and Kidney Diseases (NN), and US Public Health Service Grants (grant nos. P20 AA017067, P20 AA017067-01S1, P20 AA017067-03S1 and U01 AA021887-03) from the National Institute on Alcohol Abuse and Alcoholism (NN).

Availability of data and materials

All data generated or analyzed during this study are included in this published article.

Authors' contributions

FM was responsible for the study supervision, statistical analysis, drafting and editing of the manuscript, and data acquisition and interpretation. CCB, CLCN, AMGL, AOVA and AGMD contributed to data acquisition and editing of the manuscript. MCIC was responsible for the study design and concept, data acquisition and editing of the manuscript. NN interpreted the data, was responsible for the financial support for the study, drafting and editing the manuscript and the critical revision for important intellectual content. ARRS obtained financial support for the study, drafted and edited the manuscript, contributed to the study design and conception, critically revised the manuscript for important intellectual content and gave final approval of the version for submission. All authors read and approved the final manuscript.

Ethics approval and consent to participate

All animal studies and humane endpoints set out for this study were in accordance with the rules of Ethical and Technical Specifications for Care and Management outlined in The National Institutes of Health's Guide, and approved by Jalisco State Agency for the Care and Use of Laboratory Animals (approval no. 16/UG-JAL/2008).

Patient consent for publication

Not applicable.

Competing interests

The authors declare that they have no competing interests.

References

1. Patel D, Kumar R, Laloo D and Hemalatha S: Diabetes mellitus: An overview on its pharmacological aspects and reported medicinal plants having antidiabetic activity. Asian Pac J Trop Biomed 2: 411-420, 2012.

2. Kayama Y, Raaz U, Jagger A, Adam M, Schellinger IN, Sakamoto M, Suzuki H, Toyama K, Spin JM and Tsao PS: Diabetic cardiovascular disease induced by oxidative stress. Int J Mol Sci 16: 25234-25263, 2015.
3. Kumar S, Singh R, Vasudeva N and Sharma S: Acute and chronic animal models for the evaluation of anti-diabetic agents. Cardiovasc Diabetol 11: 9, 2012.
4. Wang HJ, Jin YX, Shen W, Neng J, Wu T, Li YJ and Fu ZW: Low dose streptozotocin (STZ) combined with high energy intake can effectively induce type 2 diabetes through altering the related gene expression. Asia Pac J Clin Nutr 16 (Suppl 1): S412-S417, 2007.
5. Malfitano C, de Souza Junior AL, Carbonaro M, Bolsoni-Lopes A, Figueroa D, de Souza LE, Silva KA, Consolim-Colombo F, Curi R and Irigoyen MC: Glucose and fatty acid metabolism in infarcted heart from streptozotocin-induced diabetic rats after 2 weeks of tissue remodeling. Cardiovasc Diabetol 14: 149, 2015.
6. Nugent DA, Smith DM and Jones HB: A review of islet of Langerhans degeneration in rodent models of type 2 diabetes. Toxicol Pathol 36: 529-551, 2008.
7. Serban AI, Stanca L, Geicu OI, Munteanu MC, Costache M and Dinischiotu A: Extracellular matrix is modulated in advanced glycation end products milieu via a RAGE receptor dependent pathway boosted by transforming growth factor-β1 RAGE. J Diabetes 7: 114-124, 2015.
8. Du AJ, Ren B, Gao XW, Yang L, Fu Y and Zhao XD: Effects of aminoguanidine on retinal apoptosis in mice with oxygen-induced retinopathy. Int J Ophthalmol 6: 436-441, 2013.
9. Serhiyenko VA and Serhiyenko AA: Diabetic cardiac autonomic neuropathy: Do we have any treatment perspectives? World J Diabetes 6: 245-258, 2015.
10. Thornalley PJ: Use of aminoguanidine (Pimagedine) to prevent the formation of advanced glycation endproducts. Arch Biochem Biophys 419: 31-40, 2003.
11. Soliman M: Preservation of myocardial contractile function by aminoguanidine, a nitric oxide synthase inhibitors, in a rat model of hemorrhagic shock. Pak J Med Sci 29: 1415-1419, 2013.
12. Niki T, Rombouts K, De Bleser P, De Smet K, Rogiers V, Schuppan D, Yoshida M, Gabbiani G and Geerts A: A histone deacetylase inhibitor, trichostatin A, suppresses myofibroblastic differentiation of rat hepatic stellate cells in primary culture. Hepatology 29: 858-867, 1999.
13. Rombouts K, Niki T, Greenwel P, Vandermonde A, Wielant A, Hellemans K, De Bleser P, Yoshida M, Schuppan D, Rojkind M and Geerts A: Trichostatin A, a histone deacetylase inhibitor, suppresses collagen synthesis and prevents TGF-beta(1)-induced fibrogenesis in skin fibroblasts. Exp Cell Res 278: 184-197, 2002.
14. Grabiec K, Gajewska M, Milewska M, Blaszczyk M and Grzelkowska-Kowalczyk K: The influence of high glucose and high insulin on mechanisms controlling cell cycle progression and arrest in mouse C2C12 myoblasts: The comparison with IGF-I effect. J Endocrinol Invest 37: 233-245, 2014.
15. Wang CC, Gurevich I and Draznin B: Insulin affects vascular smooth muscle cell phenotype and migration via distinct signaling pathways. Diabetes 52: 2562-2569, 2003.
16. Boateng SY, Hartman TJ, Ahluwalia N, Vidula H, Desai TA and Russell B: Inhibition of fibroblast proliferation in cardiac myocyte cultures by surface microtopography. Am J Physiol Cell Physiol 285: C171-C182, 2003.
17. Li M and Hagerman AE: Effect of (-)-epigallocatechin-3-gallate on glucose-induced human serum albumin glycation. Free Radic Res 49: 946-953, 2015.
18. Johnson PD and Besselsen DG: Practical aspects of experimental design in animal research. ILAR J 43: 202-206, 2002.
19. Festing MF and Altman DG: Guidelines for the design and statistical analysis of experiments using laboratory animals. ILAR J 43: 244-258, 2002.
20. Lattouf R, Younes R, Lutomski D, Naaman N, Godeau G, Senni K and Changotade S: Picrosirius red staining: A useful tool to appraise collagen networks in normal and pathological tissues. J Histochem Cytochem 62: 751-758, 2014.
21. Livak KJ and Schmittgen TD: Analysis of relative gene expression data using real-time quantitative PCR and the 2(-Delta Delta C(T)) method. Methods 25: 402-408, 2001.
22. Halban PA, Polonsky KS, Bowden DW, Hawkins MA, Ling C, Mather KJ, Powers AC, Rhodes CJ, Sussel L and Weir GC: β-cell failure in type 2 diabetes: Postulated mechanisms and prospects for prevention and treatment. J Clin Endocrinol Metab 99: 1983-1992, 2014.
23. Rao KB, Malathi N, Narashiman S and Rajan ST: Evaluation of myofibroblasts by expression of alpha smooth muscle actin: A marker in fibrosis, dysplasia and carcinoma. J Clin Diagn Res 8: ZC14-ZC17, 2014.
24. Lijnen PJ, van Pelt JF and Fagard RH: Stimulation of reactive oxygen species and collagen synthesis by angiotensin II in cardiac fibroblasts. Cardiovasc Ther 30: e1-e8, 2012.
25. Ma ZA, Zhao Z and Turk J: Mitochondrial dysfunction and β-cell failure in type 2 diabetes mellitus. Exp Diabetes Res 2012: 703538, 2012.
26. Tian XY, Wong WT, Xu A, Lu Y, Zhang Y, Wang L, Cheang WS, Wang Y, Yao X and Huang Y: Uncoupling protein-2 protects endothelial function in diet-induced obese mice. Circ Res 110: 1211-1216, 2012.
27. Parthasarathy A, Gopi V, Devi K M S, Balaji N and Vellaichamy E: Aminoguanidine inhibits ventricular fibrosis and remodeling process in isoproterenol-induced hypertrophied rat hearts by suppressing ROS and MMPs. Life Sci 118: 15-26, 2014.
28. Chowdhury P, Soulsby ME and Scott JL: Effects of aminoguanidine on tissue oxidative stress induced by hindlimb unloading in rats. Ann Clin Lab Sci 39: 64-70, 2009.
29. Cigremis Y, Parlakpinar H, Polat A, Colak C, Ozturk F, Sahna E, Ermis N and Acet A: Beneficial role of aminoguanidine on acute cardiomyopathy related to doxorubicin-treatment. Mol Cell Biochem 285: 149-154, 2006.
30. Wegner M, Neddermann D, Piorunska-Stolzmann M and Jagodzinski PP: Role of epigenetic mechanisms in the development of chronic complications of diabetes. Diabetes Res Clin Pract 105: 164-175, 2014.
31. Bertacca A, Ciccarone A, Cecchetti P, Vianello B, Laurenza I, Maffei M, Chiellini C, Del Prato S and Benzi L: Continually high insulin levels impair Akt phosphorylation and glucose transport in human myoblasts. Metabolism 54: 1687-163, 2005.
32. Lu TC, Wang ZH, Feng X, Chuang PY, Fang W, Shen Y, Levy DE, Xiong H, Chen N and He JC: Knockdown of Stat3 activity in vivo prevents diabetic glomerulopathy. Kidney Int 76: 63-71, 2009.
33. Yahiaoui L, Gvozdic D, Danialou G, Mack M and Petrof BJ: CC family chemokines directly regulate myoblast responses to skeletal muscle injury. J Physiol 586: 3991-4004, 2008.
34. Tang M, Zhang W, Lin H, Jiang H, Dai H and Zhang Y: High glucose promotes the production of collagen types I and III by cardiac fibroblasts through a pathway dependent on extracellular-signal-regulated kinase 1/2. Mol Cell Biochem 301: 109-114, 2007.
35. Dong Y, Lakhia R, Thomas SS, Dong Y, Wang XH, Silva KA and Zhang L: Interactions between p-Akt and Smad3 in injured muscles initiate myogenesis or fibrogenesis. Am J Physiol Endocrinol Metab 305: E367-E375, 2013.
36. Schiaffino S and Mammucari C: Regulation of skeletal muscle growth by the IGF1-Akt/PKB pathway: Insights from genetic models. Skelet Muscle 1: 4, 2011.
37. Sakai M, Oimomi M and Kasuga M: Experimental studies on the role of fructose in the development of diabetic complications. Kobe J Med Sci 48: 125-136, 2002.
38. Wang XL, Lau WB, Yuan YX, Wang YJ, Yi W, Christopher TA, Lopez BL, Liu HR and Ma XL: Methylglyoxal increases cardiomyocyte ischemia-reperfusion injury via glycative inhibition of thioredoxin activity. Am J Physiol Endocrinol Metab 299: E207-E214, 2010.
39. Ding WY, Liu L, Wang ZH, Tang MX, Ti Y, Han L, Zhang L, Zhang Y, Zhong M and Zhang W: FP-receptor gene silencing ameliorates myocardial fibrosis and protects from diabetic cardiomyopathy. J Mol Med (Berl) 92: 629-640, 2014.
40. Yu W, Wu J, Cai F, Xiang J, Zha W, Fan D, Guo S, Ming Z and Liu C: Curcumin alleviates diabetic cardiomyopathy in experimental diabetic rats. PLoS One7: e52013, 2012.
41. Rajesh M, Mukhopadhyay P, Bátkai S, Patel V, Saito K, Matsumoto S, Kashiwaya Y, Horváth B, Mukhopadhyay B, Becker L, *et al*: Cannabidiol attenuates cardiac dysfunction, oxidative stress, fibrosis, and inflammatory and cell death signaling pathways in diabetic cardiomyopathy. J Am Coll Cardiol 56: 2115-2125, 2010.
42. King AJ: The use of animal models in diabetes research. Br J Pharmacol 166: 877-894, 2012.
43. Zhang Y, Babcock SA, Hu N, Maris JR, Wang H and Ren J: Mitochondrial aldehyde dehydrogenase (ALDH2) protects against streptozotocin-induced diabetic cardiomyopathy: Role of GSK3β and mitochondrial function. BMC Med 10: 40, 2012.

44. Asbun J and Villarreal FJ: The pathogenesis of myocardial fibrosis in the setting of diabetic cardiomyopathy. J Am Coll Cardiol 47: 693-700, 2006.
45. Vijan S: In the clinic. Type 2 diabetes. Ann Intern Med 152: ITC31-ITC15, ITC316, 2010.
46. Ježek P, Olejár T, Smolková K, Jezek J, Dlasková A, Plecitá-Hlavatá L, Zelenka J, Špaček T, Engstová H, Pajuelo Reguera D and Jabůrek M: Antioxidant and regulatory role of mitochondrial uncoupling protein UCP2 in pancreatic beta-cells. Physiol Res 63 (Suppl 1): S73-S91, 2014.
47. Baldelli S, Aquilano K and Ciriolo MR: Punctum on two different transcription factors regulated by PGC-α: Nuclear factor erythroid-derived 2-like 2 and nuclear respiratory factor 2. Biochim Biophys Acta 1830: 4137-4146, 2013.
48. Li B, Liu S, Miao L and Cai L: Prevention of diabetic complications by activation of Nrf2: Diabetic cardiomyopathy and nephropathy. Exp Diabetes Res 2012: 216512, 2012.
49. Lassègue B and Griendling KK: NADPH oxidases: Functions and pathologies in the vasculature. Arterioscler Thromb Vasc Biol 30: 653-661, 2010.
50. Chen F, Haigh S, Barman S and Fulton DJ: From form to function: The role of Nox4 in the cardiovascular system. Front Physiol 3: 412, 2012.
51. Pendyala S and Natarajan V: Redox regulation of Nox proteins. Respir Physiol Neurobiol 174: 265-271, 2010.
52. Brewer AC, Murray TV, Arno M, Zhang M, Anilkumar NP, Mann GE and Shah AM: Nox4 regulates Nrf2 and glutathione redox in cardiomyocytes in vivo. Free Radic Biol Med 51: 205-215, 2011.
53. Dusting GJ and Triggle C: Are we over oxidized? Oxidative stress, cardiovascular disease, and the future of intervention studies with antioxidants. Vasc Health Risk Manag 1: 93-97, 2005.
54. Kazakov A, Hall R, Jagoda P, Bachelier K, Müller-Best P, Semenov A, Lammert F, Böhm M and Laufs U: Inhibition of endothelial nitric oxide synthase induces and enhances myocardial fibrosis. Cardiovasc Res 100: 211-221, 2013.
55. Oak JH, Youn JY and Cai H: Aminoguanidine inhibits aortic hydrogen peroxide production, VSMC NOX activity and hypercontractility in diabetic mice. Cardiovasc Diabetol 8: 65, 2009.
56. Li W, Cui M, Wei Y, Kong X, Tang L and Xu D: Inhibition of the expression of TGF-β1 and CTGF in human mesangial cells by exendin-4, a glucagon-like peptide-1 receptor agonist. Cell Physiol Biochem 30: 749-757, 2012.
57. Yokoi H, Kasahara M, Mori K, Kuwabara T, Toda N, Yamada R, Namoto S, Yamamoto T, Seki N, Souma N, *et al*: Peritoneal fibrosis and high transport are induced in mildly pre-injured peritoneum by 3,4-dideoxyglucosone-3-ene in mice. Perit Dial Int 33: 143-154, 2013.
58. Dhar A, Dhar I, Desai KM and Wu L: Methylglyoxal scavengers attenuate endothelial dysfunction induced by methylglyoxal and high concentrations of glucose. Br J Pharmacol 161: 1843-1856, 2010.
59. Eika B, Levin RM and Longhurst PA: Modulation of urinary bladder function by sex hormones in streptozotocin-diabetic rats. J Urol 152: 537-543, 1994.
60. Youssef S, Nguyen DT, Soulis T, Panagiotopoulos S, Jerums G and Cooper ME: Effect of diabetes and aminoguanidine therapy on renal advanced glycation end-product binding. Kidney Int 55: 907-916, 1999.
61. Wilkinson-Berka JL, Kelly DJ, Koerner SM, Jaworski K, Davis B, Thallas V and Cooper ME: ALT-946 and aminoguanidine, inhibitors of advanced glycation, improve severe nephropathy in the diabetic transgenic (mREN-2)27 rat. Diabetes 51: 3283-3289, 2002.
62. Han DC, Isono M, Hoffman BB and Ziyadeh FN: High glucose stimulates proliferation and collagen type I synthesis in renal cortical fibroblasts: Mediation by autocrine activation of TGF-beta. J Am Soc Nephrol 10: 1891-1899, 1999.
63. Aguilar H, Fricovsky E, Ihm S, Schimke M, Maya-Ramos L, Aroonsakool N, Ceballos G, Dillmann W, Villarreal F and Ramirez-Sanchez I: Role for high-glucose-induced protein O-GlcNAcylation in stimulating cardiac fibroblast collagen synthesis. Am J Physiol Cell Physiol 306: C794-C804, 2014.
64. Fiaschi T, Magherini F, Gamberi T, Lucchese G, Faggian G, Modesti A and Modesti PA: Hyperglycemia and angiotensin II cooperate to enhance collagen I deposition by cardiac fibroblasts through a ROS-STAT3-dependent mechanism. Biochim Biophys Acta 1843: 2603-2610, 2014.
65. Kojima H, Fujimiya M, Matsumura K, Nakahara T, Hara M and Chan L: Extrapancreatic insulin-producing cells in multiple organs in diabetes. Proc Natl Acad Sci USA 101: 2458-2463, 2004.
66. Phadnis SM, Ghaskadbi SM, Hardikar AA and Bhonde RR: Mesenchymal stem cells derived from bone marrow of diabetic patients portrait unique markers influenced by the diabetic microenvironment. Rev Diabet Stud 6: 260-270, 2009.
67. Wang CC, Goalstone ML and Draznin B: Molecular mechanisms of insulin resistance that impact cardiovascular biology. Diabetes 53: 2735-2740, 2004.
68. Grzebyk E and Piwowar A: Inhibitory actions of selected natural substances on formation of advanced glycation endproducts and advanced oxidation protein products. BMC Complement Altern Med 16: 381, 2016.
69. Islas-Carbajal MC, Covarrubias A, Grijalva G, Alvarez-Rodriguez A, Armendáriz-Borunda J and Rincón-Sánchez AR: Nitric oxide synthases inhibition results in renal failure improvement in cirrhotic rats. Liver Int 25: 131-140, 2005.
70. Corbett JA, Tilton RG, Chang K, Hasan KS, Ido Y, Wang JL, Sweetland MA, Lancaster JR Jr, Williamson JR and McDaniel ML: Aminoguanidine, a novel inhibitor of nitric oxide formation, prevents diabetic vascular dysfunction. Diabetes 41: 552-556, 1992.
71. Ara C, Karabulut AB, Kirimlioglu H, Yilmaz M, Kirimliglu V and Yilmaz S: Protective effect of aminoguanidine against oxidative stress in an experimental peritoneal adhesion model in rats. Cell Biochem Funct 24: 443-448, 2006.
72. Stadler K, Jenei V, Somogyi A and Jakus J: Beneficial effects of aminoguanidine on the cardiovascular system of diabetic rats. Diabetes Metab Res Rev 21: 189-196, 2005.
73. Richardson MA, Furlani RE, Podell BK, Ackart DF, Haugen JD, Melander RJ, Melander C and Basaraba RJ: Inhibition and breaking of advanced glycation end-products (AGEs) with bis-2-aminoimidazole derivatives. Tetrahedron Lett 56: 3406-3409, 2015.
74. Giardino I, Fard AK, Hatchell DL and Brownlee M: Aminoguanidine inhibits reactive oxygen species formation, lipid peroxidation, and oxidant-induced apoptosis. Diabetes 47: 1114-1120, 1998.
75. Oldfield MD, Bach LA, Forbes JM, Nikolic-Paterson D, McRobert A, Thallas V, Atkins RC, Osicka T, Jerums G and Cooper ME: Advanced glycation end products cause epithelial-myofibroblast transdifferentiation via the receptor for advanced glycation end products (RAGE). J Clin Invest 108: 1853-1863, 2001.
76. Khazaei M, Karimi J, Sheikh N, Goodarzi MT, Saidijam M, Khodadadi I and Moridi H: Effects of resveratrol on receptor for advanced glycation end products (RAGE) expression and oxidative stress in the liver of rats with type 2 diabetes. Phytother Res 30: 66-71, 2016.
77. Tan Y, Ichikawa T, Li J, Si Q, Yang H, Chen X, Goldblatt CS, Meyer CJ, Li X, Cai L and Cui T: Diabetic downregulation of Nrf2 activity via ERK contributes to oxidative stress-induced insulin resistance in cardiac cells in vitro and in vivo. Diabetes 60: 625-633, 2011.